


# Active anti-disturbance control of a quadrotor unmanned aerial vehicle using the command-filtering backstepping approach

Ahmed Aboudonia · Ayman El-Badawy  ·  
Ramy Rashad

Received: 23 October 2016 / Accepted: 17 July 2017  
© Springer Science+Business Media B.V. 2017

**Abstract** In this paper, a backstepping-based nonlinear controller is developed to control the quadrotor in the presence of constant and time-varying disturbances. The control law is derived based on Lyapunov stability arguments. The controller is integrated with a disturbance observer to estimate and attenuate the effect of the disturbing forces and moments influencing the quadrotor. In this approach, no disturbance model is required for the disturbance observer. Discontinuous terms are added to the control law to ensure the negative definiteness of the Lyapunov function derivative without neglecting the disturbance observer estimation errors. Command filtering is used to compute the derivatives of the virtual control signals to avoid the complex analytic derivation of these derivatives, and to avoid differentiating the discontinuous terms existing in the controller. The effectiveness of the developed controller is investigated in simulations against

disturbances due to partial actuator failure, wind, and unmodeled rotor dynamics.

**Keywords** Active anti-disturbance control · Command-filtering backstepping control · Disturbance observer · Quadrotor

## 1 Introduction

Quadrotors have drawn the attention of many researchers in different fields because of their wide range of applications. Unfortunately, they are found to be inherently unstable. Thus, several studies have been carried out to stabilize their dynamics and enhance their performance using different control approaches. Among the control techniques used for such purpose is the backstepping control technique.

In [5], a cascaded controller was designed such that the quadrotor model was divided into an inner loop representing the attitude dynamics and an outer loop describing the position dynamics. A backstepping controller was designed to stabilize the dynamics of each loop separately. In other words, the inner loop dynamics were ignored while designing the controller of the outer loop. In [20], a backstepping controller was designed to stabilize the quadrotor dynamics by dividing the quadrotor model into three subsystems. The first subsystem included the altitude and yaw dynamics. The second subsystem described the horizontal position dynamics together with the roll and pitch dynamics.

---

A. Aboudonia · R. Rashad  
Mechatronics Department, Faculty of Engineering and  
Materials Science, German University in Cairo, Cairo,  
Egypt

A. Aboudonia  
e-mail: ahmed.abou-donia@guc.edu.eg

R. Rashad  
e-mail: ramy.abdelmonem@guc.edu.eg

A. El-Badawy (✉)  
Mechanical Engineering Department, Al-Azhar University  
and German University in Cairo, Cairo, Egypt  
e-mail: ayman.elbadawy@guc.edu.eg

Finally, the third subsystem represented the propellers' thrust force dynamics. The same authors utilized the backstepping technique for quadrotor stabilization in [22], where the quadrotor's model was divided into three subsystems similar to [20]. However, the third subsystem in [22] represented the propellers' angular speed dynamics instead of the propellers' thrust force dynamics.

One drawback of the standard backstepping control approach is that the time derivatives of the virtual control commands are needed for the control system design. These signal derivatives can be obtained by numerical differentiation as in [20]. However, this approach is impractical due to the amplification of high frequency noise in the sensor measurements. Another method to obtain these signal derivatives is to derive them analytically as in [5]. This analytical derivation was possible due to the cascaded nature of the controller and neglecting the nonlinear transformation between the Euler rates and the body rates. However, for the full quadrotor model, the analytical derivation of these signals might be tedious. In [23], a backstepping controller was designed in such a way that the virtual control inputs and their derivatives were estimated using sliding mode differentiators. Thus, the analytic derivation of these derivatives was avoided. Another approach to avoid the analytic derivation of the virtual control inputs' derivatives is the command-filtered backstepping approach proposed by Farrell et al. [10]. This approach has been utilized to design quadrotor tracking controllers in several recent studies as in [9,39–41].

Unlike the standard backstepping approach, the command-filtering backstepping technique uses, in each step, a filtered signal of the virtual control input instead of the actual one. The filtered signal is obtained by propagating the actual signal through a low-pass filter. This filter provides the derivative of the filtered signal as well. This derivative is used together with the filtered signal instead of the derivative of the actual signal. Thus, the differentiation of the actual signal is no longer needed. In this approach, the compensated tracking error is defined, in each step, to be the difference between the tracking error in this step and an auxiliary variable. This auxiliary variable is mainly added to cancel the error between the actual virtual control signal and its filtered version and, thus, to prove the stability of the compensated tracking error.

Another drawback of using the backstepping technique to design quadrotor control systems is the lack

of robustness to disturbances that may be applied to the quadrotor during flight. These disturbances may be exogenous such as those due to wind, whereas others may be endogenous such as the ones due to parameter uncertainties and unmodeled dynamics. Several approaches are developed to provide backstepping-based controllers with robustness against disturbances.

These techniques can be divided into passive anti-disturbance control (PADC) techniques and active anti-disturbance control (AADC) techniques [19]. Starting with the passive anti-disturbance techniques, these are the techniques that attenuate disturbances through feedback control. These approaches include, but not limited to, integral control [19], adaptive control [2], and sliding mode control [17]. In integral control, an integral term is added to the controller to attenuate the effect of disturbances as is the case with PID control which was applied to quadrotors in [4,18]. In adaptive control, the parameters of the controller are determined based on estimated model parameters, and thus, this control scheme deals effectively with parameter uncertainties. Adaptive control was extensively used in the domain of quadrotor control [11,27,33,34]. In sliding mode control, a control law is designed so that a sliding surface is reached in finite time. After reaching the sliding surface, a reduced-order model is obtained whose state trajectories slide along the sliding surface toward the origin. To attenuate the disturbances influencing the quadrotor using sliding mode control, this control scheme requires the upper bounds of these disturbances. Sliding mode control was applied to the quadrotor as found in [5,38].

All the above-mentioned PADC were combined with the backstepping-based control in several studies to enhance its robustness. In [31], an integral backstepping controller with command filtering was implemented on a quadrotor to handle constant disturbances and unmodeled actuator dynamics. In [16], an adaptive backstepping controller was designed to control the quadrotor in the presence of uncertain model parameters, more specifically, unknown quadrotor mass parameter. In [21], a sliding mode controller was augmented with the backstepping-based controller to attenuate the effect of disturbances. In [24], a sliding mode observer was integrated with the backstepping-based controller to estimate the unmeasured states as well as the disturbances affecting the quadrotor. Other PADC schemes can be found in the first chapter in [19].

As mentioned in [19], although disturbances are finally canceled through passive anti-disturbance controllers, they are rejected in a relatively slow manner. Thus, active anti-disturbance control methods are utilized to get over the PADC limitations. Active anti-disturbance control relies on disturbance estimates to cancel the effect of the actual disturbances through feedforward compensation. This control technique includes, but not limited to, disturbance observer-based control (DOBC) and active disturbance rejection control (ADRC). In active disturbance rejection control, an augmented state vector is created combining the system's states and disturbances. An extended state observer is designed to estimate the new augmented vector including the states and the disturbances. Active disturbance rejection control was extensively investigated in the literature as shown in [12, 13, 29, 30]. In disturbance observer-based control, disturbance estimates are given using the so-called disturbance observer that was, first, introduced in [26]. Since then, different structures of disturbance observers have been utilized and applied to quadrotors, such as the sliding mode disturbance observer in [3], the nonlinear disturbance observer in [36] and the frequency-domain disturbance observer in [14]. An overview on the different active anti-disturbance control techniques is found in [8].

Recently, some efforts have been carried out to provide robustness to the backstepping-based controllers by combining them with disturbance observers as in [35] in which the disturbances were considered to be constant, at steady state, for the convenience of the stability analysis. Furthermore, in [7], a backstepping controller was integrated with a disturbance observer for the purpose of quadrotor control. Nevertheless, neither the command-filtering technique nor the sliding mode differentiators were used to overcome the problem of differentiating the virtual control inputs of the backstepping controller. Moreover, a disturbance model was utilized within the controller to reject the effect of the applied disturbances. In a recent study, a disturbance observer-based backstepping controller has been proposed in [32]. The proposed control scheme combined the backstepping technique based on the command-filtering approach with a disturbance observer and was applied to a laboratory setup called the twin-rotor MIMO system. The boundedness of the tracking error signals was proven using singular perturbation theory. In this approach, the disturbance observer estimation

errors were neglected in the Lyapunov stability analysis. Neglecting the disturbance observer estimation errors was valid since the disturbance observer dynamics was selected to be much faster than the applied disturbances.

The main aim of this paper is to control the quadrotor in the presence of both constant and time-varying disturbances, unlike [35]. The proposed controller is based on the command-filtering backstepping technique and derived using Lyapunov stability arguments. Robustness against disturbances is achieved via the active anti-disturbance scheme in which a nonlinear disturbance observer is used to estimate the disturbing forces and moments without utilizing an internal model for them. The absence of an internal model leads to the existence of disturbance observer estimation errors that may result in the indefiniteness of the Lyapunov function derivative. Thus, discontinuous terms are added to ensure the negative definiteness of the Lyapunov function derivative without neglecting the disturbance observer estimation errors, unlike the approach in [32]. Finally, the command-filtered backstepping approach is used to compute the derivatives of the associated command signals, unlike [7]. The advantage of this modified approach is twofold: First one is to avoid the complex analytic derivation of these derivatives and to avoid using numerical differentiation. The second one is to avoid the numerical differentiation of the discontinuous terms existing in the controller. The proposed controller is assessed by applying it in simulations to a quadrotor model in the presence of time-varying wind disturbances and partial actuator failure. The wind model comprises constant wind, discrete wind gust, and Dryden wind. However, partial actuator failure is simulated by modifying the thrust force produced by one of the propellers at a specific speed to be less than those produced by the others at the same angular speed. Moreover, the proposed controller is compared to the controller developed in [32] in the presence of unmodeled rotor dynamics which are represented by first-order linear filters.

The paper is organized as follows: The dynamic model of the quadrotor, including partial actuator failure as well as wind disturbances, is introduced in Sect. 2. In Sect. 3, the disturbance observer-based command-filtering backstepping controller is developed. Finally, the simulation results are presented in Sect. 4, followed by the conclusion in Sect. 5.

## 2 Dynamic model

The quadrotor equations of motion have been derived and investigated in various studies [25, 28]. The quadrotor is a MIMO underactuated nonlinear system having four control inputs and six degrees of freedom. The four control inputs are the total thrust  $U_1$ , the rolling moment  $U_2$ , the pitching moment  $U_3$ , and the yawing moment  $U_4$ . The six degrees of freedom include the quadrotor attitude  $\Theta = (\phi \ \theta \ \psi)^\top$  and the quadrotor position  $\mathbf{P} = (x \ y \ z)^\top$ . In this section, the quadrotor kinematics and dynamics are introduced.

### 2.1 Translational kinematics and dynamics

In order to derive the translational kinematics, two reference frames are defined. The first one is the inertial reference frame  $I : \{O_I, X_I, Y_I, Z_I\}$  which is fixed to the ground, whereas the second one is the body-fixed reference frame  $B : \{O_B, X_B, Y_B, Z_B\}$  whose origin is attached to the quadrotor center of mass and whose axes rotate with the quadrotor. Denoting  $\phi$ ,  $\theta$  and  $\psi$  as the roll, pitch, and yaw angles representing the quadrotor attitude, the rotation matrix  $\mathbf{R}$  converting the body-fixed frame axes to the inertial frame axes is expressed as

$$\mathbf{R} = \begin{bmatrix} c_\theta c_\psi & s_\phi s_\theta c_\psi - c_\phi s_\psi & c_\phi s_\theta c_\psi + s_\phi s_\psi \\ c_\theta s_\psi & s_\phi s_\theta s_\psi + c_\phi c_\psi & c_\phi s_\theta s_\psi - s_\phi c_\psi \\ s_\theta & s_\phi c_\theta & c_\phi c_\theta \end{bmatrix}. \quad (1)$$

where  $s_{(\cdot)}$  represents the sine function and  $c_{(\cdot)}$  represents the cosine function.

Based on the Newton–Euler equations of motion, the translational dynamics, represented in the inertial frame, are described as

$$m\ddot{\mathbf{P}} = \mathbf{F}, \quad (2)$$

where  $m$  is the mass of the quadrotor,  $\mathbf{F}$  is the total force affecting the quadrotor and comprises three main forces. These forces are the disturbing force  $\mathbf{F}_d = [d_x \ d_y \ d_z]^\top$  which will be derived in detail in the coming subsections, and the thrust force  $\mathbf{F}_t$  and the gravitational force  $\mathbf{F}_g$  are given, respectively, by

$$\mathbf{F}_t = U_1 \mathbf{R} \bar{\mathbf{e}}_3, \quad \mathbf{F}_g = -mg \bar{\mathbf{e}}_3, \quad (3)$$

where  $g$  is the gravitational acceleration,  $\bar{\mathbf{e}}_3 = [0 \ 0 \ 1]^\top$ . Since the collective thrust  $U_1$  is directed in the positive direction of the  $Z_B$  axis, this thrust is multiplied by the vector  $\bar{\mathbf{e}}_3$ . Then, it is multiplied by the rotation matrix  $\mathbf{R}$  to be converted to the inertial reference frame. Similarly, since the gravitational force is directed in the negative direction of  $Z_I$  axis, this force is multiplied by the vector  $-\bar{\mathbf{e}}_3$ . The disturbing force is considered to be already represented in the inertial frame. Therefore, the total force vector is represented as

$$\begin{aligned} \mathbf{F} &= \mathbf{F}_t + \mathbf{F}_g + \mathbf{F}_d \\ &= U_1 \mathbf{R} \bar{\mathbf{e}}_3 - mg \bar{\mathbf{e}}_3 + \mathbf{F}_d \end{aligned} \quad (4)$$

By substituting (4) in (2), the quadrotor translational dynamics is represented in detailed form as

$$\begin{bmatrix} \ddot{x} \\ \ddot{y} \\ \ddot{z} \end{bmatrix} = \begin{bmatrix} (s_\phi s_\psi + c_\phi s_\theta c_\psi) \frac{U_1}{m} + \frac{d_x}{m} \\ (-s_\phi c_\psi + c_\phi s_\theta s_\psi) \frac{U_1}{m} + \frac{d_y}{m} \\ c_\phi c_\theta \frac{U_1}{m} - g + \frac{d_z}{m} \end{bmatrix}, \quad (5)$$

The disturbing forces  $d_x$ ,  $d_y$  and  $d_z$  are divided into two parts: the wind forces  $d_{wx}$ ,  $d_{wy}$  and  $d_{wz}$  and the partial actuator failure forces  $d_{ux}$ ,  $d_{uy}$  and  $d_{uz}$  as follows

$$\begin{bmatrix} d_x \\ d_y \\ d_z \end{bmatrix} = \begin{bmatrix} d_{wx} + d_{ux} \\ d_{wy} + d_{uy} \\ d_{wz} + d_{uz} \end{bmatrix}. \quad (6)$$

### 2.2 Rotational kinematics and dynamics

As for the rotational kinematics, the relation between the quadrotor angular velocities  $\boldsymbol{\Omega} = [p \ q \ r]^\top$  and the Euler rates  $\dot{\Theta} = [\dot{\phi} \ \dot{\theta} \ \dot{\psi}]^\top$  is described as

$$\begin{bmatrix} \dot{\phi} \\ \dot{\theta} \\ \dot{\psi} \end{bmatrix} = \begin{bmatrix} 1 & s_\phi t_\theta & c_\phi t_\theta \\ 0 & c_\phi & -s_\phi \\ 0 & s_\phi / c_\theta & c_\phi / c_\theta \end{bmatrix} \begin{bmatrix} p \\ q \\ r \end{bmatrix}. \quad (7)$$

where  $t_{(\cdot)}$  represents the tangent function. Based on the Newton–Euler equations of motion, the rotational dynamics are described as

$$\mathbf{I} \dot{\boldsymbol{\Omega}} = -\boldsymbol{\Omega} \times \mathbf{I} \boldsymbol{\Omega} + \mathbf{M} \quad (8)$$

where the symbol  $(\times)$  denotes the cross product of two vectors,  $\mathbf{I} = \text{diag}\{I_x, I_y, I_z\}$  is the inertia matrix of

the quadrotor, and  $\mathbf{M}$  is the total torque vector including two main torques. These torques are the disturbing torques  $\mathbf{D}_m = [d_{up} \ d_{uq} \ d_{ur}]$  and the input torques  $\mathbf{U}_m = [U_2 \ U_3 \ U_4]^T$ . Thus, the total torque vector is written as

$$\mathbf{M} = \mathbf{U}_m + \mathbf{D}_m. \quad (9)$$

By substituting (9) in (8), the quadrotor rotational dynamics is represented in detailed form as

$$\begin{bmatrix} \dot{p} \\ \dot{q} \\ \dot{r} \end{bmatrix} = \begin{bmatrix} \frac{1}{I_x} [(I_y - I_z)qr + U_2 + d_{up}] \\ \frac{1}{I_y} [(I_z - I_x)pr + U_3 + d_{uq}] \\ \frac{1}{I_z} [(I_x - I_y)pq + U_4 + d_{ur}] \end{bmatrix}, \quad (10)$$

The only source of disturbing moments  $d_k$ ,  $k \in \{p, q, r\}$ , introduced in this work, is the moment due to the partial actuator failure  $d_{uk}$  and thus

$$d_p = d_{up}, \quad d_q = d_{uq}, \quad d_r = d_{ur} \quad (11)$$

The disturbances due to wind and partial actuator failure are discussed in details in the following subsections.

### 2.3 Wind disturbance model

The wind model utilized in this paper is introduced in this subsection and follows [1]. The inertial wind velocities  $v_{wx}$ ,  $v_{wy}$ , and  $v_{wz}$  are produced due to the following contributions:

1. Constant wind in which the velocity of the wind remains unchanged.
2. Discrete wind gust [6, 15] in which the wind velocity changes from a certain value  $\bar{v}_{wj1}$  at time  $t_1$  to another value  $\bar{v}_{wj2}$  at time  $t_2$  using the following rule

$$\bar{v}_{wj} = \bar{v}_{wj1} + \frac{(\bar{v}_{wj2} - \bar{v}_{wj1})}{2} \left( 1 - \cos \left( \frac{\pi(t - t_1)}{t_2 - t_1} \right) \right), \quad (12)$$

3. Dryden wind model [15, 37] in which the wind velocity is produced by transmitting band-limited white noise through the linear filters

$$\begin{aligned} G_x(s) &= \sigma_x \sqrt{\frac{2L_x}{\pi V}} \frac{1}{1 + \frac{L_x}{V}s} \\ G_y(s) &= \sigma_y \sqrt{\frac{L_y}{\pi V}} \frac{1 + \frac{\sqrt{3}L_y}{V}s}{(1 + \frac{L_y}{V}s)^2}, \\ G_z(s) &= \sigma_z \sqrt{\frac{L_z}{\pi V}} \frac{1 + \frac{\sqrt{3}L_z}{V}s}{(1 + \frac{L_z}{V}s)^2} \end{aligned} \quad (13)$$

where  $V$  is the quadrotor speed,  $s$  is the Laplace variable,  $\sigma_k$  and  $L_k$ ,  $k \in \{x, y, z\}$ , are the turbulence intensities and scale lengths, respectively, given by

$$\begin{aligned} \sigma_z &= 0.1W_6, \quad L_z = z, \\ \sigma_x &= \frac{\sigma_w}{(0.177 + 0.000823z)^{0.4}}, \quad L_x = \frac{z}{(0.177 + 0.000823z)^{1.2}} \\ \sigma_y &= \frac{\sigma_w}{(0.177 + 0.000823z)^{0.4}}, \quad L_y = \frac{z}{(0.177 + 0.000823z)^{1.2}} \end{aligned} \quad (14)$$

where  $W_6$  denotes the wind speed at an altitude of 6 m.

The generated wind influences the quadrotor in the form of a drag force  $d_w$  as follows. Let  $v_j$  and  $v_{wj}$  represent the quadrotor and wind velocities, respectively, with respect to ground. Denoting  $\rho$  as the air density,  $C_{dj}$  as the quadrotor drag coefficient along the inertial axis  $j$  and  $A_j$  as the projected quadrotor area in a plane perpendicular to the inertial axis  $j$ , the drag force components  $d_{wj}$ ,  $j \in \{x, y, z\}$ , are expressed as,

$$d_{wj} = -0.5\rho C_{dj} A_j (v_j - v_{wj})^2 \text{sgn}(v_j - v_{wj}), \quad (15)$$

where  $\text{sgn}(\cdot)$  denotes the sign function and the area  $\mathbf{A}_i = [A_x \ A_y \ A_z]^T$  is computed as follows,

$$\mathbf{A}_i = \hat{\mathbf{R}} \mathbf{A}_b, \quad (16)$$

where  $\mathbf{A}_b = [A_u \ A_v \ A_w]^T$  is a vector including the projected quadrotor areas in the body-fixed planes and  $\hat{\mathbf{R}}$  is a matrix whose elements represent the absolute values of the corresponding elements in the rotation matrix  $\mathbf{R}$ .

### 2.4 Actuator failure uncertainties

A partial actuator failure is modeled by considering that the thrust force produced by the failed rotor, at a

particular angular speed, reaches a value lower than the required one. To model this effect, we assume that only the front rotor is damaged without loss of generality. Denoting  $\lambda$  as the degree of effectiveness of the front rotor, the relation between the actual inputs  $\bar{U}_i$  acting on the quadrotor's rigid body and the calculated ones  $U_i$  is given by

$$\begin{bmatrix} \bar{U}_1 \\ \bar{U}_2 \\ \bar{U}_3 \\ \bar{U}_4 \end{bmatrix} = \begin{bmatrix} \frac{3+\lambda}{4} & 0 & \frac{1-\lambda}{2l_a} & \frac{b-b\lambda}{4d} \\ 0 & 1 & 0 & 0 \\ \frac{l_a-l_a\lambda}{4} & 0 & \frac{1+\lambda}{2} & \frac{bl_a(-1+\lambda)}{4d} \\ \frac{d-d\lambda}{4b} & 0 & \frac{d(-1+\lambda)}{2bl_a} & \frac{3+\lambda}{4} \end{bmatrix} \begin{bmatrix} U_1 \\ U_2 \\ U_3 \\ U_4 \end{bmatrix}. \quad (17)$$

where  $b$  and  $d$  are the thrust and drag coefficients respectively,  $l_a$  is the distance between the rotor's center of rotation and the quadrotor center. The detailed derivation of (17) can be found in [1]. The disturbing force along the thrust force direction, in this case, is given by

$$d_{u1} = \bar{U}_1 - U_1, \quad (18)$$

and can be resolved along the inertial axes as follows

$$\begin{aligned} d_{ux} &= (s_\phi s_\psi + c_\phi s_\theta c_\psi) d_{u1}, \\ d_{uy} &= (-s_\phi c_\psi + c_\phi s_\theta s_\psi) d_{u1}, \\ d_{uz} &= (c_\phi c_\theta) d_{u1}. \end{aligned} \quad (19)$$

On the other hand, the disturbing moments are

$$\begin{aligned} d_{up} &= d_{u2} = \bar{U}_2 - U_2, \\ d_{uq} &= d_{u3} = \bar{U}_3 - U_3, \\ d_{ur} &= d_{u4} = \bar{U}_4 - U_4. \end{aligned} \quad (20)$$

## 2.5 State space model

In this subsection, a quadrotor state space model is introduced. The states of this model are selected to be

$$\begin{aligned} \mathbf{x}_1 &= \begin{bmatrix} x \\ y \end{bmatrix}, \mathbf{x}_3 = \begin{bmatrix} \phi \\ \theta \end{bmatrix}, \mathbf{x}_5 = \begin{bmatrix} z \\ \psi \end{bmatrix}, \\ \mathbf{x}_2 &= \begin{bmatrix} \dot{x} \\ \dot{y} \end{bmatrix}, \mathbf{x}_4 = \begin{bmatrix} p \\ q \end{bmatrix}, \mathbf{x}_6 = \begin{bmatrix} \dot{z} \\ r \end{bmatrix}, \end{aligned} \quad (21)$$

Whereas the control inputs are chosen to be

$$\mathbf{u}_1 = \begin{bmatrix} U_2 \\ U_3 \end{bmatrix}, \mathbf{u}_2 = \begin{bmatrix} U_1 \\ U_4 \end{bmatrix}, \quad (22)$$

Finally, the disturbances are selected to be

$$\begin{aligned} \mathbf{d}_1 &= \begin{bmatrix} d_x \\ d_y \end{bmatrix} = \begin{bmatrix} d_{wx} + d_{ux} \\ d_{wy} + d_{uy} \end{bmatrix}, \\ \mathbf{d}_2 &= \begin{bmatrix} d_p \\ d_q \end{bmatrix} = \begin{bmatrix} d_{up} \\ d_{uq} \end{bmatrix}, \\ \mathbf{d}_3 &= \begin{bmatrix} d_z \\ d_r \end{bmatrix} = \begin{bmatrix} d_{wz} + d_{uz} \\ d_{ur} \end{bmatrix}, \end{aligned} \quad (23)$$

where  $d_{wx}$ ,  $d_{wy}$  and  $d_{wz}$  are the disturbing forces due to wind given by (15),  $d_{ux}$ ,  $d_{uy}$ ,  $d_{uz}$ ,  $d_{up}$ ,  $d_{uq}$  and  $d_{ur}$  are the disturbing forces and moments due to partial actuator failure. In this case, using (5, 7, 10), the quadrotor nonlinear state space model is written in the form

$$\dot{\mathbf{x}} = \mathbf{f}(\mathbf{x}, \mathbf{u}) + \mathbf{B}_d \mathbf{d} \quad (24)$$

as follows

$$\begin{aligned} \begin{bmatrix} \dot{\mathbf{x}}_1 \\ \dot{\mathbf{x}}_2 \\ \dot{\mathbf{x}}_3 \\ \dot{\mathbf{x}}_4 \\ \dot{\mathbf{x}}_5 \\ \dot{\mathbf{x}}_6 \end{bmatrix} &= \begin{bmatrix} \mathbf{x}_2 \\ \mathbf{g}_2(\mathbf{x}_5, U_1) \mathbf{w}(\mathbf{x}_3) \\ \mathbf{f}_3(\mathbf{x}_3, \mathbf{x}_6) + \mathbf{g}_3(\mathbf{x}_3) \mathbf{x}_4 \\ \mathbf{f}_4(\mathbf{x}_4) + \mathbf{g}_4 \mathbf{u}_1 \\ \mathbf{f}_5(\mathbf{x}_3, \mathbf{x}_4) + \mathbf{g}_5(\mathbf{x}_3) \mathbf{x}_6 \\ \mathbf{f}_6(\mathbf{x}_4) + \mathbf{g}_6(\mathbf{x}_3) \mathbf{u}_2 \end{bmatrix} \\ &+ \begin{bmatrix} 0_2 & 0_2 & 0_2 \\ \mathbf{h}_2 & 0_2 & 0_2 \\ 0_2 & 0_2 & 0_2 \\ 0_2 & \mathbf{h}_4 & 0_2 \\ 0_2 & 0_2 & 0_2 \\ 0_2 & 0_2 & \mathbf{h}_6 \end{bmatrix} \begin{bmatrix} \mathbf{d}_1 \\ \mathbf{d}_2 \\ \mathbf{d}_3 \end{bmatrix} \end{aligned} \quad (25)$$

where

$$\begin{aligned} \mathbf{g}_2 &= \frac{U_1}{m} \begin{bmatrix} s_\psi & c_\psi \\ -c_\psi & s_\psi \end{bmatrix}, \mathbf{w} = \begin{bmatrix} s_\phi \\ c_\phi s_\theta \end{bmatrix}, \mathbf{h}_2 = \begin{bmatrix} \frac{1}{m} & 0 \\ 0 & \frac{1}{m} \end{bmatrix}, \\ \mathbf{f}_3 &= \begin{bmatrix} c_\phi t_\theta r \\ -s_\phi r \end{bmatrix}, \mathbf{g}_3 = \begin{bmatrix} 1 & s_\phi t_\theta \\ 0 & c_\phi \end{bmatrix}, \\ \mathbf{f}_4 &= \begin{bmatrix} \frac{I_y - I_z}{I_x} q r \\ \frac{I_z - I_x}{I_y} p r \end{bmatrix}, \mathbf{g}_4 = \begin{bmatrix} \frac{1}{I_x} & 0 \\ 0 & \frac{1}{I_y} \end{bmatrix}, \mathbf{h}_4 = \begin{bmatrix} \frac{1}{I_x} & 0 \\ 0 & \frac{1}{I_y} \end{bmatrix}, \\ \mathbf{f}_5 &= \begin{bmatrix} 0 \\ (s_\phi / c_\theta) q \end{bmatrix}, \mathbf{g}_5 = \begin{bmatrix} 1 & 0 \\ 0 & c_\phi / c_\theta \end{bmatrix}, \\ \mathbf{f}_6 &= \begin{bmatrix} -g \\ \frac{I_x - I_y}{I_z} p q \end{bmatrix}, \mathbf{g}_6 = \begin{bmatrix} \frac{c_\psi c_\theta}{m} & 0 \\ 0 & \frac{1}{I_z} \end{bmatrix}, \mathbf{h}_6 = \begin{bmatrix} \frac{1}{m} & 0 \\ 0 & \frac{1}{I_z} \end{bmatrix}. \end{aligned} \quad (26)$$



The state space model in (25) is the quadrotor model to be used to design the backstepping controller.

### 3 Control system design

In this section, the controller design is divided into two parts. First, a disturbance observer is designed to find estimates for the disturbing forces and moments influencing the quadrotor. Then, a command-filtering backstepping controller is designed utilizing the disturbance estimates obtained by the disturbance observer.

#### 3.1 Disturbance observer

The disturbance observer uses the quadrotor model states and inputs to estimate the actual disturbances. These estimates are then used to suppress the influence of the disturbances while designing the backstepping controller. The disturbance observer, designed in this work, follows [19] and is represented as

$$\begin{aligned}\dot{\mathbf{z}} &= -\mathbf{L}\mathbf{B}_d\mathbf{z} - \mathbf{L}(\mathbf{f}(\mathbf{x}, \mathbf{u}) + \mathbf{B}_d\mathbf{L}\mathbf{x}), \\ \hat{\mathbf{d}} &= \mathbf{z} + \mathbf{L}\mathbf{x},\end{aligned}\quad (27)$$

where  $\mathbf{z}$  is the state vector of the disturbance observer,  $\mathbf{L}$  is the gain matrix of the disturbance observer and  $\hat{\mathbf{d}}$  is the disturbance estimate vector. The error dynamics of the disturbance observer is given by

$$\dot{\mathbf{e}}_d = -\mathbf{L}\mathbf{B}_d\mathbf{e}_d + \dot{\mathbf{d}}, \quad (28)$$

where  $\mathbf{e}_d$  is the difference between the actual disturbance vector and the disturbance estimate vector. By designing the matrix  $\mathbf{L}$  to be

$$\mathbf{L} = \mathbf{L}_d\mathbf{B}_d^+, \quad (29)$$

where  $\mathbf{B}_d^+ = (\mathbf{B}_d^\top \mathbf{B}_d)^{-1} \mathbf{B}_d^\top$  is the left pseudo-inverse of  $\mathbf{B}_d$  and  $\mathbf{L}_d = \text{diag}(l_{d1}, \dots, l_{d6})$  is a positive definite diagonal matrix, the error dynamics is modified to be

$$\dot{\mathbf{e}}_d = -\mathbf{L}_d\mathbf{e}_d + \dot{\mathbf{d}}. \quad (30)$$

Since the matrix  $\mathbf{L}_d$  is assumed to be a positive definite matrix, then the disturbance observer error dynamics is stable. Using the definition of the disturbance observer

estimation error, rearranging the error dynamics in (30) results in the following equation

$$\dot{\hat{\mathbf{d}}} = -\mathbf{L}_d\hat{\mathbf{d}} + \mathbf{L}_d\mathbf{d}. \quad (31)$$

From (31), it can be inferred that the disturbance estimate  $\hat{d}_i$  of a certain disturbance  $d_i$  is the output of a unity-DC-gain first-order low-pass filter whose input is the disturbance  $d_i$ . Thus, this disturbance observer can estimate the constant wind disturbances at steady state. As for discrete wind gust, this wind type results due to sinusoidal wind velocity. Thus, the higher the bandwidth of the disturbance observer given by  $\mathbf{L}_d$  with respect to the frequency of the wind velocity, the lower the disturbance observer estimation error. Finally, the Dryden wind gust results due to the propagation of band-limited white noise through the low-pass filters given in (13). Similarly, the higher the disturbance observer bandwidth with respect to the filter's bandwidth of the Dryden wind, the lower the disturbance observer estimation error. The occurrence of the disturbance observer estimation errors due to the different kinds of disturbances is handled while designing the feedback controller in the next subsection.

#### 3.2 Backstepping controller design

In this section, the command-filtering backstepping-based controller is developed. To design the backstepping-based controller, the quadrotor model is divided into two subsystems. The first subsystem describes the altitude and yaw dynamics and includes the states  $\mathbf{x}_5$  and  $\mathbf{x}_6$ . While the second subsystem describes the horizontal position dynamics and includes the states  $\mathbf{x}_1$ ,  $\mathbf{x}_2$ ,  $\mathbf{x}_3$  and  $\mathbf{x}_4$ .

##### 3.2.1 Horizontal position control

The horizontal position controller is divided into four steps as shown below.

###### Horizontal Position Step 1:

First, a virtual control input  $\mathbf{v}_1$  is defined such that

$$\dot{\mathbf{x}}_1 = \mathbf{v}_1. \quad (32)$$

In addition, the position tracking error  $\mathbf{z}_{1,1}$  is defined to be

$$\mathbf{z}_{1,1} = \hat{\mathbf{x}}_{1d} - \mathbf{x}_1 \quad (33)$$

where  $\hat{\mathbf{x}}_{1d}$  is a filtered version of the desired horizontal position trajectory  $\mathbf{x}_{1d}$  obtained by propagating the actual trajectory  $\mathbf{x}_{1d}$  through the low-pass filter with the transfer function

$$H_1(s) = \frac{a_{10}}{s^2 + a_{11}s + a_{10}} \quad (34)$$

such that  $a_{11} > 0$  and  $a_{10} > 0$  are the filter gains. To guarantee the stability in this step, a Lyapunov function  $V_1$  is defined to be

$$V_1 = \frac{1}{2} \mathbf{z}_{1,1}^\top \mathbf{z}_{1,1} \quad (35)$$

Using (32, 33), the derivative of the Lyapunov function  $V_1$  is found to be

$$\dot{V}_1 = \mathbf{z}_{1,1}^\top \dot{\mathbf{z}}_{1,1} = \mathbf{z}_{1,1}^\top (\dot{\hat{\mathbf{x}}}_{1d} - \mathbf{v}_1) \quad (36)$$

By designing the virtual control input  $\mathbf{v}_1$  to be

$$\mathbf{v}_1 = \dot{\hat{\mathbf{x}}}_{1d} + \mathbf{K}_1 \mathbf{z}_{1,1}, \quad (37)$$

where  $\mathbf{K}_1 = k_1 \mathbf{I}_{2 \times 2}$  with  $k_1 > 0$ , the above Lyapunov function derivative is modified to be

$$\dot{V}_1 = -\mathbf{z}_{1,1}^\top \mathbf{K}_1 \mathbf{z}_{1,1}, \quad (38)$$

proving the stabilization of the position tracking error  $\mathbf{z}_{1,1}$  in this step. In this case, assuming the virtual control signal  $\mathbf{v}_1$  as the control input, the horizontal position vector  $\mathbf{x}_1$  converges to the filtered version of the desired trajectory  $\hat{\mathbf{x}}_{1d}$  which follows the desired trajectory  $\mathbf{x}_{1d}$ .

*Horizontal Position Step 2:*

Second, a virtual control input  $\mathbf{v}_2$  is defined such that

$$\dot{\mathbf{x}}_2 = \mathbf{g}_2 \mathbf{v}_2 + \mathbf{h}_2 \mathbf{d}_1. \quad (39)$$

Moreover, the velocity tracking error  $\mathbf{z}_{2,1}$  is defined to be

$$\mathbf{z}_{2,1} = \hat{\mathbf{v}}_1 - \mathbf{x}_2 \quad (40)$$

where  $\hat{\mathbf{v}}_1$  is a filtered version obtained by passing the virtual control input  $\mathbf{v}_1$  through the command-filtering

low-pass filter with the transfer function

$$H_2(s) = \frac{a_{20}}{s^2 + a_{21}s + a_{20}}. \quad (41)$$

such that  $a_{21} > 0$  and  $a_{20} > 0$  are the filter gains. From (33, 37, 40), the derivative of the tracking error  $\mathbf{z}_{1,1}$  is given by

$$\begin{aligned} \dot{\mathbf{z}}_{1,1} &= \dot{\hat{\mathbf{x}}}_{1d} - \dot{\mathbf{x}}_1 \\ &= -\mathbf{K}_1 \mathbf{z}_{1,1} + \mathbf{v}_1 - \mathbf{x}_2 \\ &= -\mathbf{K}_1 \mathbf{z}_{1,1} + \hat{\mathbf{v}}_1 - \mathbf{x}_2 + \mathbf{v}_1 - \hat{\mathbf{v}}_1 \\ &= -\mathbf{K}_1 \mathbf{z}_{1,1} + \mathbf{z}_{2,1} + \mathbf{v}_1 - \hat{\mathbf{v}}_1 \end{aligned} \quad (42)$$

To guarantee the stability in the second step, a Lyapunov function  $V_2$  is defined as

$$V_2 = \frac{1}{2} \mathbf{z}_{1,2}^\top \mathbf{z}_{1,2} + \frac{1}{2} \mathbf{z}_{2,1}^\top \mathbf{z}_{2,1} \quad (43)$$

where  $\mathbf{z}_{1,2} = \mathbf{z}_{1,1} - \mathbf{w}_{1,1}$  is a compensated tracking error and  $\mathbf{w}_{1,1}$  is an auxiliary control variable. Using (39, 40, 42), the derivative of the Lyapunov function  $V_2$  is found to be

$$\begin{aligned} \dot{V}_2 &= \mathbf{z}_{1,2}^\top (\dot{\mathbf{z}}_{1,1} - \dot{\mathbf{w}}_{1,1}) + \mathbf{z}_{2,1}^\top \dot{\mathbf{z}}_{2,1} \\ &= \mathbf{z}_{1,2}^\top (-\mathbf{K}_1 \mathbf{z}_{1,1} + \mathbf{z}_{2,1} + \mathbf{v}_1 - \hat{\mathbf{v}}_1 - \dot{\mathbf{w}}_{1,1}) \\ &\quad + \mathbf{z}_{2,1}^\top (\hat{\mathbf{v}}_1 - \mathbf{g}_2 \mathbf{v}_2 - \mathbf{h}_2 \mathbf{d}_1) \\ &= \mathbf{z}_{1,2}^\top (-\mathbf{K}_1 \mathbf{z}_{1,1} + \mathbf{v}_1 - \hat{\mathbf{v}}_1 - \dot{\mathbf{w}}_{1,1}) \\ &\quad + \mathbf{z}_{2,1}^\top (\hat{\mathbf{v}}_1 + \mathbf{z}_{1,2} - \mathbf{g}_2 \mathbf{v}_2 - \mathbf{h}_2 \mathbf{d}_1) \end{aligned} \quad (44)$$

Design the virtual control input  $\mathbf{v}_2$  and the auxiliary variable  $\mathbf{w}_{1,1}$  dynamics to be

$$\begin{aligned} \mathbf{v}_2 &= \mathbf{g}_2^{-1} \left( \dot{\hat{\mathbf{v}}}_1 + \mathbf{z}_{1,2} + \mathbf{K}_2 \mathbf{z}_{2,1} + \mathbf{L}_2 \text{sgn}(\mathbf{z}_{2,1}) - \mathbf{h}_2 \hat{\mathbf{d}}_1 \right), \\ \dot{\mathbf{w}}_{1,1} &= -\mathbf{K}_1 \mathbf{w}_{1,1} + \mathbf{v}_1 - \hat{\mathbf{v}}_1, \end{aligned} \quad (45)$$

where  $\mathbf{K}_2 = k_2 \mathbf{I}_{2 \times 2}$  and  $\mathbf{L}_2 = l_2 \mathbf{I}_{2 \times 2}$  are control gain matrices,  $\hat{\mathbf{d}}_1$  is the estimate of the disturbance  $\mathbf{d}_1$  and  $\text{sgn}(\mathbf{z}_{2,1})$  is a vector whose  $i$ th entry represents the sign of the  $i$ th entry of the vector  $\mathbf{z}_{2,1}$ . Notice that the matrix  $\mathbf{g}_2$  is invertible in (45) if and only if  $U_1 \neq 0$  which is satisfied in normal flight conditions. Denote  $\mathbf{e}_1 = \mathbf{d}_1 - \hat{\mathbf{d}}_1$  as the disturbance observer estimation error of the disturbance  $\mathbf{d}_1$ . By substituting the virtual control input and the auxiliary variable expressions (45)



in the Lyapunov function derivative (44), the Lyapunov function derivative is written as

$$\begin{aligned}\dot{V}_2 = & -\mathbf{z}_{1,2}^\top \mathbf{K}_1 \mathbf{z}_{1,2} - \mathbf{z}_{2,1}^\top \mathbf{K}_2 \mathbf{z}_{2,1} \\ & - \mathbf{z}_{2,1}^\top \mathbf{L}_2 \text{sgn}(\mathbf{z}_{2,1}) - \mathbf{z}_{2,1}^\top \mathbf{h}_2 \mathbf{e}_1,\end{aligned}\quad (46)$$

To prove the stabilization of the velocity tracking error  $\mathbf{z}_2$  in this step, the negative definiteness of the Lyapunov function derivative has to be ensured. By choosing the gain  $k_2 > 0$  and since  $k_1 > 0$ , the first two terms in (46) are found to be negative definite due to their quadratic nature. Using the definition of  $\mathbf{h}_2$  in (26), the last two terms can be expressed, respectively, as

$$\begin{aligned}\mathbf{z}_{2,1}^\top \mathbf{L}_2 \text{sgn}(\mathbf{z}_{2,1}) &= l_2(|z_{2,1(1)}| + |z_{2,1(2)}|) \\ \mathbf{z}_{2,1}^\top \mathbf{h}_2 \mathbf{e}_1 &= \frac{e_{1(1)}}{m} z_{2,1(1)} + \frac{e_{1(2)}}{m} z_{2,1(2)}\end{aligned}\quad (47)$$

where

$$\mathbf{z}_{2,1} = \begin{bmatrix} z_{2,1(1)} \\ z_{2,1(2)} \end{bmatrix} \quad \mathbf{e}_2 = \begin{bmatrix} e_{1(1)} \\ e_{1(2)} \end{bmatrix}\quad (48)$$

In order to ensure the negative definiteness of the summation of the two terms in (47), the gain  $l_2$  is chosen to be always higher than the larger value of  $e_{1(1)}/m$  and  $e_{1(2)}/m$ . In other words, the gain  $l_2$  is chosen to be always higher than the infinity norm of the vector  $\mathbf{e}_1/m$ . Let  $\mathbf{e}_{1,\max}$  be a vector whose entries represent the upper bounds of the corresponding entries in the vector  $\mathbf{e}_1$  and denote  $\|(\cdot)\|_\infty$  as the infinity norm. Therefore, the following conditions

$$k_2 > 0, \quad l_2 > \|\mathbf{h}_2 \mathbf{e}_{1,\max}\|_\infty \quad (49)$$

ensure the negative definiteness of the Lyapunov function derivative in (46). In this case, assuming the virtual control signal  $\mathbf{v}_2$  as the control input, the quadrotor horizontal velocity  $\mathbf{x}_2$  converges to the filtered version of the virtual control input  $\hat{\mathbf{v}}_1$  which follows the virtual control input  $\mathbf{v}_1$ .

*Horizontal Position Step 3:*

Third, a virtual control input  $\mathbf{v}_3$  is defined such that

$$\dot{\mathbf{x}}_3 = \mathbf{f}_3 + \mathbf{g}_3 \mathbf{v}_3. \quad (50)$$

Moreover, the roll and pitch step tracking error  $\mathbf{z}_{3,1}$  is defined to be

$$\mathbf{z}_{3,1} = \hat{\mathbf{v}}_2 - \mathbf{w} \quad (51)$$

where  $\hat{\mathbf{v}}_2$  is a filtered version of the virtual control input  $\mathbf{v}_2$  obtained using the command-filtering low-pass filter

$$H_3(s) = \frac{a_{30}}{s^2 + a_{31}s + a_{30}}. \quad (52)$$

such that  $a_{31} > 0$  and  $a_{30} > 0$  are the filter gains. Using (40, 45, 51), the derivative of the tracking error  $\mathbf{z}_{2,1}$  is found to be

$$\begin{aligned}\dot{\mathbf{z}}_{2,1} &= \dot{\hat{\mathbf{v}}}_1 - \dot{\mathbf{x}}_2 \\ &= -\mathbf{K}_2 \mathbf{z}_{2,1} - \mathbf{z}_{1,2} + \mathbf{g}_2 \mathbf{v}_2 - \mathbf{L}_2 \text{sgn}(\mathbf{z}_{2,1}) \\ &\quad + \mathbf{h}_2 \hat{\mathbf{d}}_1 - \mathbf{g}_2 \mathbf{w} - \mathbf{h}_2 \mathbf{d}_1 \\ &= -\mathbf{K}_2 \mathbf{z}_{2,1} - \mathbf{z}_{1,2} + \mathbf{g}_2 \hat{\mathbf{v}}_2 - \mathbf{g}_2 \mathbf{w} + \mathbf{g}_2 \mathbf{v}_2 - \mathbf{g}_2 \hat{\mathbf{v}}_2 \\ &\quad - \mathbf{L}_2 \text{sgn}(\mathbf{z}_{2,1}) - \mathbf{h}_2 \mathbf{e}_1 \\ &= -\mathbf{K}_2 \mathbf{z}_{2,1} - \mathbf{z}_{1,2} + \mathbf{g}_2 \mathbf{z}_{3,1} + \mathbf{g}_2 (\mathbf{v}_2 - \hat{\mathbf{v}}_2) \\ &\quad - \mathbf{L}_2 \text{sgn}(\mathbf{z}_{2,1}) - \mathbf{h}_2 \mathbf{e}_1\end{aligned}\quad (53)$$

To prove the stability in this step, a Lyapunov function  $V_3$  is defined to be

$$V_3 = \frac{1}{2} \mathbf{z}_{1,3}^\top \mathbf{z}_{1,3} + \frac{1}{2} \mathbf{z}_{2,2}^\top \mathbf{z}_{2,2} + \frac{1}{2} \mathbf{z}_{3,1}^\top \mathbf{z}_{3,1} \quad (54)$$

where  $\mathbf{z}_{1,3} = \mathbf{z}_{1,2} - \mathbf{w}_{1,2}$  and  $\mathbf{z}_{2,2} = \mathbf{z}_{2,1} - \mathbf{w}_{2,1}$  are compensated tracking errors and  $\mathbf{w}_{1,2}$  and  $\mathbf{w}_{2,1}$  are auxiliary control variables. Using (42, 45, 50, 51, 53), the derivative of the Lyapunov function  $V_3$  is found to be

$$\begin{aligned}\dot{V}_3 &= \mathbf{z}_{1,3}^\top (\dot{\mathbf{z}}_{1,1} - \dot{\mathbf{w}}_{1,1} - \dot{\mathbf{w}}_{1,2}) \\ &\quad + \mathbf{z}_{2,2}^\top (\dot{\mathbf{z}}_{2,1} - \dot{\mathbf{w}}_{2,1}) + \mathbf{z}_{3,1}^\top \dot{\mathbf{z}}_{3,1} \\ &= \mathbf{z}_{1,3}^\top \left( -\mathbf{K}_1 \mathbf{z}_{1,1} + \mathbf{z}_{2,1} + \mathbf{v}_1 - \hat{\mathbf{v}}_1 \right. \\ &\quad \left. + \mathbf{K}_1 \mathbf{w}_{1,1} - \mathbf{v}_1 + \hat{\mathbf{v}}_1 - \dot{\mathbf{w}}_{1,2} \right) \\ &\quad + \mathbf{z}_{2,2}^\top \left( -\mathbf{K}_2 \mathbf{z}_{2,1} - \mathbf{z}_{1,2} + \mathbf{g}_2 \mathbf{z}_{3,1} + \mathbf{g}_2 (\mathbf{v}_2 - \hat{\mathbf{v}}_2) \right. \\ &\quad \left. - \mathbf{L}_2 \text{sgn}(\mathbf{z}_{2,1}) - \mathbf{h}_2 \mathbf{e}_1 - \dot{\mathbf{w}}_{2,1} \right) \\ &\quad + \mathbf{z}_{3,1}^\top \left( \dot{\hat{\mathbf{v}}}_2 - \frac{\partial \mathbf{w}}{\partial \mathbf{x}_3} \dot{\mathbf{x}}_3 \right) \\ &= \mathbf{z}_{1,3}^\top (-\mathbf{K}_1 \mathbf{z}_{1,1} + \mathbf{K}_1 \mathbf{w}_{1,1} + \mathbf{z}_{2,1} - \dot{\mathbf{w}}_{1,2}) \\ &\quad + \mathbf{z}_{2,2}^\top \left( -\mathbf{K}_2 \mathbf{z}_{2,1} - \mathbf{z}_{1,2} + \mathbf{g}_2 \mathbf{z}_{3,1} + \mathbf{g}_2 (\mathbf{v}_2 - \hat{\mathbf{v}}_2) \right. \\ &\quad \left. - \mathbf{L}_2 \text{sgn}(\mathbf{z}_{2,1}) - \mathbf{h}_2 \mathbf{e}_1 - \dot{\mathbf{w}}_{2,1} \right)\end{aligned}$$

$$+ \mathbf{z}_{3,1}^\top (\dot{\hat{\mathbf{v}}}_2 - \frac{\partial \mathbf{w}}{\partial \mathbf{x}_3} \mathbf{f}_3 - \frac{\partial \mathbf{w}}{\partial \mathbf{x}_3} \mathbf{g}_3 \mathbf{v}_3) \quad (55)$$

where  $\frac{\partial \mathbf{w}}{\partial \mathbf{x}_3}$  denotes the partial derivative of the vector  $\mathbf{w}$  with respect to the vector  $\mathbf{x}_3$ . By designing the virtual control input  $\mathbf{v}_3$  and the auxiliary variables  $\mathbf{w}_{1,2}$  and  $\mathbf{w}_{2,1}$  dynamics to be

$$\begin{aligned} \mathbf{v}_3 &= \left( \frac{\partial \mathbf{w}}{\partial \mathbf{x}_3} \mathbf{g}_3 \right)^{-1} (\dot{\hat{\mathbf{v}}}_2 + \mathbf{g}_2^\top \mathbf{z}_{2,2} - \frac{\partial \mathbf{w}}{\partial \mathbf{x}_3} \mathbf{f}_3 + \mathbf{K}_3 \mathbf{z}_{3,1}), \\ \dot{\mathbf{w}}_{1,2} &= -\mathbf{K}_1 \mathbf{w}_{1,2} + \mathbf{w}_{2,1} \\ \dot{\mathbf{w}}_{2,1} &= -\mathbf{K}_2 \mathbf{w}_{2,1} - \mathbf{w}_{1,2} + \mathbf{g}_2 (\mathbf{v}_2 - \hat{\mathbf{v}}_2) \\ &\quad - \mathbf{L}_2 \text{sgn}(\mathbf{z}_{2,1}) + \mathbf{L}_2 \text{sgn}(\mathbf{z}_{2,2}) \end{aligned} \quad (56)$$

where  $\mathbf{K}_3 = k_3 \mathbf{I}_{2 \times 2}$  with  $k_3 > 0$ , the above Lyapunov function derivative is modified to be

$$\begin{aligned} \dot{V}_3 &= -\mathbf{z}_{1,3}^\top \mathbf{K}_1 \mathbf{z}_{1,3} - \mathbf{z}_{2,2}^\top \mathbf{K}_2 \mathbf{z}_{2,2} - \mathbf{z}_{2,2}^\top \mathbf{L}_2 \text{sgn}(\mathbf{z}_{2,2}) \\ &\quad - \mathbf{z}_{2,2}^\top \mathbf{h}_2 \mathbf{e}_1 - \mathbf{z}_{3,1}^\top \mathbf{K}_3 \mathbf{z}_{3,1}, \end{aligned} \quad (57)$$

guaranteeing the stability of the third step tracking error  $\mathbf{z}_3$  in this step. Notice that the matrix  $(\frac{\partial \mathbf{w}}{\partial \mathbf{x}_3}) \mathbf{g}_3$  is invertible if  $-\frac{\pi}{2} < \phi < \frac{\pi}{2}$  and  $-\frac{\pi}{2} < \theta < \frac{\pi}{2}$  which are satisfied in normal flight conditions. Therefore, assuming the virtual control signal  $\mathbf{v}_3$  as the control input, the vector  $\mathbf{w}$  converges to the filtered version of the virtual control input  $\hat{\mathbf{v}}_2$  which follows the virtual control input  $\mathbf{v}_2$ .

#### Horizontal Position Step 4:

Fourth, the angular velocities' tracking error  $\mathbf{z}_{4,1}$  is defined to be

$$\mathbf{z}_{4,1} = \hat{\mathbf{v}}_3 - \mathbf{x}_4 \quad (58)$$

where  $\hat{\mathbf{v}}_3$  is a filtered version of the signal  $\mathbf{v}_3$  obtained using the command-filtering low-pass filter with the transfer function

$$H_4(s) = \frac{a_{40}}{s^2 + a_{41}s + a_{40}}. \quad (59)$$

such that  $a_{41} > 0$  and  $a_{40} > 0$  are the filter gains. From (51, 56, 58), the derivative of the tracking error  $\mathbf{z}_{3,1}$  is found to be

$$\begin{aligned} \dot{\mathbf{z}}_{3,1} &= \dot{\hat{\mathbf{v}}}_2 - \dot{\mathbf{w}} \\ &= \frac{\partial \mathbf{w}}{\partial \mathbf{x}_3} \mathbf{g}_3 \mathbf{v}_3 + \frac{\partial \mathbf{w}}{\partial \mathbf{x}_3} \mathbf{f}_3 - \mathbf{g}_2^\top \mathbf{z}_{2,2} \\ &\quad - \mathbf{K}_3 \mathbf{z}_{3,1} - \frac{\partial \mathbf{w}}{\partial \mathbf{x}_3} \mathbf{f}_3 - \frac{\partial \mathbf{w}}{\partial \mathbf{x}_3} \mathbf{g}_3 \mathbf{x}_4 \\ &= \frac{\partial \mathbf{w}}{\partial \mathbf{x}_3} \mathbf{g}_3 \mathbf{v}_3 - \mathbf{g}_2^\top \mathbf{z}_{2,2} - \mathbf{K}_3 \mathbf{z}_{3,1} - \frac{\partial \mathbf{w}}{\partial \mathbf{x}_3} \mathbf{g}_3 \mathbf{x}_4 \\ &= -\mathbf{K}_3 \mathbf{z}_{3,1} - \mathbf{g}_2^\top \mathbf{z}_{2,2} + \frac{\partial \mathbf{w}}{\partial \mathbf{x}_3} \mathbf{g}_3 (\hat{\mathbf{v}}_3 - \mathbf{x}_4) \\ &\quad - \frac{\partial \mathbf{w}}{\partial \mathbf{x}_3} \mathbf{g}_3 (\mathbf{v}_3 - \hat{\mathbf{v}}_3) \\ &= -\mathbf{K}_3 \mathbf{z}_{3,1} - \mathbf{g}_2^\top \mathbf{z}_{2,2} + \left( \frac{\partial \mathbf{w}}{\partial \mathbf{x}_3} \mathbf{g}_3 \right) \hat{\mathbf{z}}_{4,1} \\ &\quad + \left( \frac{\partial \mathbf{w}}{\partial \mathbf{x}_3} \mathbf{g}_3 \right) (\mathbf{v}_3 - \hat{\mathbf{v}}_3) \end{aligned} \quad (60)$$

To prove the stability in the fourth step, the Lyapunov function  $V_4$  is defined to be

$$V_4 = \frac{1}{2} \mathbf{z}_{1,4}^\top \mathbf{z}_{1,4} + \frac{1}{2} \mathbf{z}_{2,3}^\top \mathbf{z}_{2,3} + \frac{1}{2} \mathbf{z}_{3,2}^\top \mathbf{z}_{3,2} + \frac{1}{2} \mathbf{z}_{4,1}^\top \mathbf{z}_{4,1} \quad (61)$$

where  $\mathbf{z}_{1,4} = \mathbf{z}_{1,3} - \mathbf{w}_{1,3}$ ,  $\mathbf{z}_{2,3} = \mathbf{z}_{2,2} - \mathbf{w}_{2,2}$  and  $\mathbf{z}_{3,2} = \mathbf{z}_{3,1} - \mathbf{w}_{3,1}$  are compensated tracking errors and  $\mathbf{w}_{1,3}$ ,  $\mathbf{w}_{2,2}$  and  $\mathbf{w}_{3,1}$  are auxiliary control variables. Using (25, 42, 45, 53, 56, 58, 60), the derivative of the Lyapunov function  $V_4$  is found to be

$$\begin{aligned} \dot{V}_4 &= \mathbf{z}_{1,4}^\top \dot{\mathbf{z}}_{1,4} + \mathbf{z}_{2,3}^\top \dot{\mathbf{z}}_{2,3} + \mathbf{z}_{3,2}^\top \dot{\mathbf{z}}_{3,2} + \mathbf{z}_{4,1}^\top \dot{\mathbf{z}}_{4,1} \\ &= \mathbf{z}_{1,4}^\top \left( -\mathbf{K}_1 \mathbf{z}_{1,1} + \mathbf{z}_{2,1} + \mathbf{v}_1 - \hat{\mathbf{v}}_1 + \mathbf{K}_1 \mathbf{w}_{1,1} - \mathbf{v}_1 + \hat{\mathbf{v}}_1 + \mathbf{K}_1 \mathbf{w}_{1,2} - \mathbf{w}_{2,1} - \dot{\mathbf{w}}_{1,3} \right) \\ &\quad + \mathbf{z}_{2,3}^\top \left( -\mathbf{K}_2 \mathbf{z}_{2,1} - \mathbf{L}_2 \text{sgn}(\mathbf{z}_{2,1}) - \mathbf{h}_2 \mathbf{e}_1 - \mathbf{z}_{1,2} + \mathbf{g}_2 \mathbf{z}_{3,1} + \mathbf{g}_2 (\mathbf{v}_2 - \hat{\mathbf{v}}_2) + \mathbf{K}_2 \mathbf{w}_{2,1} + \mathbf{w}_{1,2} - \mathbf{g}_2 (\mathbf{v}_2 - \hat{\mathbf{v}}_2) - \mathbf{L}_2 \text{sgn}(\mathbf{z}_{2,2}) + \mathbf{L}_2 \text{sgn}(\mathbf{z}_{2,1}) - \dot{\mathbf{w}}_{2,2} \right) \\ &\quad + \mathbf{z}_{3,2}^\top \left( -\mathbf{K}_3 \mathbf{z}_{3,1} - \mathbf{g}_2^\top \mathbf{z}_{2,2} + \frac{\partial \mathbf{w}}{\partial \mathbf{x}_3} \mathbf{g}_3 \mathbf{z}_{4,1} + \frac{\partial \mathbf{w}}{\partial \mathbf{x}_3} \mathbf{g}_3 (\mathbf{v}_3 - \hat{\mathbf{v}}_3) - \dot{\mathbf{w}}_{3,1} \right) \\ &\quad + \mathbf{z}_{4,1}^\top (\dot{\hat{\mathbf{v}}}_3 - \mathbf{f}_4 - \mathbf{g}_4 \mathbf{u}_1 - \mathbf{h}_4 \mathbf{d}_2) \\ &= \mathbf{z}_{1,4}^\top \left( -\mathbf{K}_1 \mathbf{z}_{1,1} + \mathbf{K}_1 \mathbf{w}_{1,1} + \mathbf{K}_1 \mathbf{w}_{1,2} + \mathbf{z}_{2,1} - \mathbf{w}_{2,1} - \dot{\mathbf{w}}_{1,3} \right) \\ &\quad + \mathbf{z}_{2,3}^\top \left( -\mathbf{K}_2 \mathbf{z}_{2,1} + \mathbf{K}_2 \mathbf{w}_{2,1} - \mathbf{L}_2 \text{sgn}(\mathbf{z}_{2,2}) - \mathbf{h}_2 \mathbf{e}_1 + \mathbf{g}_2 \mathbf{z}_{3,1} - \mathbf{z}_{1,2} + \mathbf{w}_{1,2} - \dot{\mathbf{w}}_{2,2} \right) \\ &\quad + \mathbf{z}_{3,2}^\top \left( -\mathbf{K}_3 \mathbf{z}_{3,1} - \mathbf{g}_2^\top \mathbf{z}_{2,2} + \frac{\partial \mathbf{w}}{\partial \mathbf{x}_3} \mathbf{g}_3 \mathbf{z}_{4,1} + \frac{\partial \mathbf{w}}{\partial \mathbf{x}_3} \mathbf{g}_3 (\mathbf{v}_3 - \hat{\mathbf{v}}_3) - \dot{\mathbf{w}}_{3,1} \right) \\ &\quad + \mathbf{z}_{4,1}^\top (\dot{\hat{\mathbf{v}}}_3 - \mathbf{f}_4 - \mathbf{g}_4 \mathbf{u}_1 - \mathbf{h}_4 \mathbf{d}_2) \end{aligned} \quad (62)$$

Design the control input  $\mathbf{u}_1$  and the auxiliary variables  $\mathbf{w}_{1,3}$ ,  $\mathbf{w}_{2,2}$  and  $\mathbf{w}_{3,1}$  dynamics as follows

$$\begin{aligned}\mathbf{u}_1 &= \mathbf{g}_4^{-1} \left( \dot{\hat{\mathbf{v}}}_3 + \left( \frac{\partial \mathbf{w}}{\partial \mathbf{x}_3} \mathbf{g}_3 \right)^\top \mathbf{z}_{3,2} - \mathbf{f}_4 - \mathbf{h}_4 \hat{\mathbf{d}}_2 \right. \\ &\quad \left. + \mathbf{K}_4 \mathbf{z}_{4,1} + \mathbf{L}_4 \text{sgn}(\mathbf{z}_{4,1}) \right), \\ \dot{\mathbf{w}}_{1,3} &= -\mathbf{K}_1 \mathbf{w}_{1,3} + \mathbf{w}_{2,2} \\ \dot{\mathbf{w}}_{2,2} &= -\mathbf{K}_2 \mathbf{w}_{2,2} + \mathbf{g}_2 \mathbf{w}_{3,1} - \mathbf{w}_{1,3} \\ &\quad - \mathbf{L}_2 \text{sgn}(\mathbf{z}_{2,2}) + \mathbf{L}_2 \text{sgn}(\mathbf{z}_{2,3}) \\ \dot{\mathbf{w}}_{3,1} &= -\mathbf{K}_3 \mathbf{w}_{3,1} + \frac{\partial \mathbf{w}}{\partial \mathbf{x}_3} \mathbf{g}_3 (\mathbf{v}_3 - \hat{\mathbf{v}}_3) - \mathbf{g}_2^\top \mathbf{w}_{2,2} \quad (63)\end{aligned}$$

where  $\mathbf{K}_4 = k_4 \mathbf{I}_{2 \times 2}$  and  $\mathbf{L}_4 = l_4 \mathbf{I}_{2 \times 2}$  are control gain matrices,  $\hat{\mathbf{d}}_2$  is the estimate of the disturbance  $\mathbf{d}_2$ , and  $\text{sgn}(\mathbf{z}_{4,1})$  is a vector whose  $i$ th entry represents the sign of the  $i$ th entry of the vector  $\mathbf{z}_{4,1}$ . Notice that the matrix  $\mathbf{g}_4$  is always invertible since it is a diagonal matrix with  $I_x$  and  $I_y$  along its diagonal. Denote  $\mathbf{e}_2 = \mathbf{d}_2 - \hat{\mathbf{d}}_2$  as the disturbance observer estimation error of the disturbance  $\mathbf{d}_2$ . By substituting the virtual control input and the auxiliary variable expressions (63) in the Lyapunov function derivative (62), the Lyapunov function derivative is modified to be

$$\begin{aligned}\dot{V}_4 &= -\mathbf{z}_{1,4}^\top \mathbf{K}_1 \mathbf{z}_{1,4} - \mathbf{z}_{2,3}^\top \mathbf{K}_2 \mathbf{z}_{2,3} \\ &\quad - \mathbf{z}_{2,3}^\top \mathbf{L}_2 \text{sgn}(\mathbf{z}_{2,3}) - \mathbf{z}_{2,3}^\top \mathbf{h}_2 \mathbf{e}_1 \\ &\quad - \mathbf{z}_{3,2}^\top \mathbf{K}_3 \mathbf{z}_{3,2} - \mathbf{z}_{4,1}^\top \mathbf{K}_4 \mathbf{z}_{4,1} \\ &\quad - \mathbf{z}_{4,1}^\top \mathbf{L}_4 \text{sgn}(\mathbf{z}_{4,1}) - \mathbf{z}_{4,1}^\top \mathbf{h}_4 \mathbf{e}_2,\end{aligned} \quad (64)$$

Recall the definition of the vector  $\mathbf{h}_4$  in (26). To prove the stabilization of the angular velocity tracking error  $\mathbf{z}_{4,1}$  in this step, the same procedures at the end of step 2 are followed leading to the conditions

$$k_4 > 0, \quad l_4 > \|\mathbf{h}_4 \mathbf{e}_{2,\max}\|_\infty, \quad (65)$$

where  $\mathbf{e}_{2,\max}$  is a vector whose entries represent the upper bounds of the corresponding entries in the vector  $\mathbf{e}_2$ . In this case, the quadrotor horizontal velocity  $\mathbf{x}_4$  converges to the filtered version of the virtual control input  $\hat{\mathbf{v}}_3$  which follows the virtual control input  $\mathbf{v}_3$ .

### 3.2.2 Altitude and heading controller

Regarding the altitude and heading controller, it is divided into two steps as shown below.

#### Altitude and Heading Step 1:

First, a virtual control input  $\mathbf{v}_5$  is defined such that

$$\dot{\mathbf{x}}_5 = \mathbf{f}_5 + \mathbf{g}_5 \mathbf{v}_5. \quad (66)$$

Moreover, the tracking error  $\mathbf{z}_{5,1}$  is defined to be

$$\mathbf{z}_{5,1} = \hat{\mathbf{x}}_{5d} - \mathbf{x}_5 \quad (67)$$

where  $\hat{\mathbf{x}}_{5d}$  is a filtered version of the desired altitude and heading trajectories  $\mathbf{x}_{5d}$  obtained by propagating the actual trajectories  $\mathbf{x}_{5d}$  through the low-pass filter

$$H_5(s) = \frac{a_{50}}{s^2 + a_{51}s + a_{50}} \quad (68)$$

where the gains  $a_{51} > 0$  and  $a_{50} > 0$  are the filter gains. To guarantee the stability in this step, the Lyapunov function  $V_5$  is chosen as

$$V_5 = \frac{1}{2} \mathbf{z}_{5,1}^\top \mathbf{z}_{5,1} \quad (69)$$

Using (66, 67), the derivative of the Lyapunov function  $V_5$  is found to be

$$\dot{V}_5 = \mathbf{z}_{5,1}^\top \dot{\mathbf{z}}_{5,1} = \mathbf{z}_{5,1}^\top (\dot{\hat{\mathbf{x}}}_{5d} - \mathbf{f}_5 - \mathbf{g}_5 \mathbf{v}_5) \quad (70)$$

By designing the virtual control input  $\mathbf{v}_5$  to be

$$\mathbf{v}_5 = \mathbf{g}_5^{-1} (\dot{\hat{\mathbf{x}}}_{5d} - \mathbf{f}_5 + \mathbf{K}_5 \mathbf{z}_{5,1}), \quad (71)$$

where  $\mathbf{K}_5 = k_5 \mathbf{I}_{2 \times 2}$  with  $k_5 > 0$ , the above Lyapunov function derivative is modified to be

$$\dot{V}_5 = -\mathbf{z}_{5,1}^\top \mathbf{K}_5 \mathbf{z}_{5,1}, \quad (72)$$

which proves the stabilization of the tracking error  $\mathbf{z}_{5,1}$  in this step. The matrix  $\mathbf{g}_5$  is invertible if  $-\frac{\pi}{2} < \phi < \frac{\pi}{2}$  which is satisfied in normal operating conditions. Notice that this condition is also reached in the horizontal position controller. In this case, assuming the virtual control signal  $\mathbf{v}_5$  as the control input, the altitude and heading vector  $\mathbf{x}_5$  converges to the filtered version of the desired trajectory  $\hat{\mathbf{x}}_{5d}$  which follows the desired trajectory  $\mathbf{x}_{5d}$ .

#### Altitude and Heading Step 2:

Second, the tracking error  $\mathbf{z}_{6,1}$  is defined to be

$$\mathbf{z}_{6,1} = \hat{\mathbf{v}}_5 - \mathbf{x}_6 \quad (73)$$

where  $\hat{\mathbf{v}}_5$  is a filtered version obtained by passing the virtual control input  $\mathbf{v}_5$  through the command-filtering low-pass filter

$$H_6(s) = \frac{a_{60}}{s^2 + a_{61}s + a_{60}} \quad (74)$$

such that  $a_{61} > 0$  and  $a_{60} > 0$  are the filter gains. From (67, 71, 73), the derivative of the tracking error  $\mathbf{z}_{5,1}$  is found to be

$$\begin{aligned} \dot{\mathbf{z}}_{5,1} &= \dot{\hat{\mathbf{x}}}_{5d} - \dot{\hat{\mathbf{x}}}_5 \\ &= -\mathbf{K}_5 \mathbf{z}_{5,1} + \mathbf{f}_5 + \mathbf{g}_5 \mathbf{v}_5 - \mathbf{f}_5 - \mathbf{g}_5 \mathbf{x}_6 \\ &= -\mathbf{K}_5 \mathbf{z}_{5,1} + \mathbf{g}_5 \hat{\mathbf{v}}_5 - \mathbf{g}_5 \mathbf{x}_6 + \mathbf{g}_5 \mathbf{v}_5 - \mathbf{g}_5 \hat{\mathbf{v}}_5 \\ &= -\mathbf{K}_5 \mathbf{z}_{5,1} + \mathbf{g}_5 \mathbf{z}_{6,1} + \mathbf{g}_5 (\mathbf{v}_5 - \hat{\mathbf{v}}_5) \end{aligned} \quad (75)$$

To prove the stability in the sixth step, the Lyapunov function  $V_6$  is defined to be

$$V_6 = \frac{1}{2} \mathbf{z}_{5,2}^\top \mathbf{z}_{5,2} + \frac{1}{2} \mathbf{z}_{6,1}^\top \mathbf{z}_{6,1} \quad (76)$$

where  $\mathbf{z}_{5,2} = \mathbf{z}_{5,1} - \mathbf{w}_{5,1}$  is a compensated tracking error and  $\mathbf{w}_{5,1}$  is an auxiliary control variable. Using (25, 73, 75), the derivative of the Lyapunov function  $V_6$  is found to be

$$\begin{aligned} \dot{V}_6 &= \mathbf{z}_{5,2}^\top \dot{\mathbf{z}}_{5,2} + \mathbf{z}_{6,1}^\top \dot{\mathbf{z}}_{6,1} \\ &= \mathbf{z}_{5,2}^\top (\dot{\mathbf{z}}_{5,1} - \dot{\mathbf{w}}_{5,1}) + \mathbf{z}_{6,1}^\top (\dot{\hat{\mathbf{v}}}_5 - \dot{\hat{\mathbf{x}}}_6) \\ &= \mathbf{z}_{5,2}^\top (-\mathbf{K}_5 \mathbf{z}_{5,1} + \mathbf{g}_5 \mathbf{z}_{6,1} + \mathbf{g}_5 (\mathbf{v}_5 - \hat{\mathbf{v}}_5) - \dot{\mathbf{w}}_{5,1}) \\ &\quad + \mathbf{z}_{6,1}^\top (\dot{\hat{\mathbf{v}}}_5 - \mathbf{f}_6 - \mathbf{g}_6 \mathbf{u}_2 - \mathbf{h}_6 \mathbf{d}_3) \end{aligned} \quad (77)$$

Design the control input  $\mathbf{u}_2$  and the auxiliary variable  $\mathbf{w}_{5,1}$  dynamics to be

$$\begin{aligned} \mathbf{u}_2 &= \mathbf{g}_6^{-1} \left( \dot{\hat{\mathbf{v}}}_5 + \mathbf{g}_5^\top \mathbf{z}_{5,2} - \mathbf{f}_6 - \mathbf{h}_6 \hat{\mathbf{d}}_3 \right. \\ &\quad \left. + \mathbf{K}_6 \mathbf{z}_{6,1} + \mathbf{L}_6 \text{sgn}(\mathbf{z}_{6,1}) \right) \\ \dot{\mathbf{w}}_{5,1} &= -\mathbf{K}_5 \mathbf{w}_{5,1} + \mathbf{g}_5 (\mathbf{v}_5 - \hat{\mathbf{v}}_5), \end{aligned} \quad (78)$$

where  $\mathbf{K}_6 = k_6 \mathbf{I}_{2 \times 2}$  and  $\mathbf{L}_6 = l_6 \mathbf{I}_{2 \times 2}$  are control gain matrices,  $\hat{\mathbf{d}}_3$  is the estimate of the disturbance  $\mathbf{d}_3$  and  $\text{sgn}(\mathbf{z}_{6,1})$  is a vector whose  $i$ th entry represents the sign of the  $i$ th entry of the vector  $\mathbf{z}_{6,1}$ . Notice that the matrix  $\mathbf{g}_6$  in (78) is invertible if and only if  $-\frac{\pi}{2} < \phi < \frac{\pi}{2}$  and  $-\frac{\pi}{2} < \theta < \frac{\pi}{2}$  which are satisfied in normal flight conditions. Denote  $\mathbf{e}_3 = \mathbf{d}_3 - \hat{\mathbf{d}}_3$  as the disturbance

observer estimation error of the disturbance  $\mathbf{d}_3$ . By substituting the virtual control input and the auxiliary variable expressions (78) in the Lyapunov function derivative (77), the Lyapunov function derivative is modified to be

$$\begin{aligned} \dot{V}_6 &= -\mathbf{z}_{5,2}^\top \mathbf{K}_5 \mathbf{z}_{5,2} - \mathbf{z}_{6,1}^\top \mathbf{K}_6 \mathbf{z}_{6,1} \\ &\quad - \mathbf{z}_{6,1}^\top \mathbf{h}_6 \mathbf{e}_3 - \mathbf{z}_{6,1}^\top \mathbf{L}_6 \text{sgn}(\mathbf{z}_{6,1}), \end{aligned} \quad (79)$$

Recall the definition of the vector  $\mathbf{h}_6$  in (26). To prove the stabilization of the tracking error  $\mathbf{z}_{6,1}$  in this step, the same procedures at the end of step 2 and step 4 of the horizontal position control are followed leading to the conditions

$$k_6 > 0, \quad l_6 > \|\mathbf{h}_6 \mathbf{e}_{3,\max}\|_\infty, \quad (80)$$

where  $\mathbf{e}_{3,\max}$  is a vector whose entries represent the upper bounds of the corresponding entries in the vector  $\mathbf{e}_3$ . In this case, the state vector  $\mathbf{x}_6$  converges to the filtered version of the virtual control input  $\hat{\mathbf{v}}_5$  which follows the virtual control input  $\mathbf{v}_5$ .

### 3.3 Main result

Finally, the main result of this work is summarized in this section. This result mainly depends on the fourth step of the horizontal position control design as well as the second step of the altitude and heading control design and can be summarized as follows.

**Theorem** Consider the quadrotor model given in (24, 25, 26). Define the compensated tracking error vector  $\mathbf{z}_c = [\mathbf{z}_{1,4}^\top, \mathbf{z}_{2,3}^\top, \mathbf{z}_{3,2}^\top, \mathbf{z}_{5,2}^\top]^\top$  and the tracking error vector  $\mathbf{z} = [\mathbf{z}_{4,1}^\top, \mathbf{z}_{6,1}^\top]^\top$  as in (61, 76). Then, the horizontal position control law (37, 45, 56, 63) and the altitude and heading control law (71, 78) together with the low-pass filters (34, 41, 52, 59, 68, 74) stabilize the compensated tracking errors  $\mathbf{z}_c$  and the tracking errors  $\mathbf{z}$ , when the gains  $k_i > 0$ ,  $i \in \{1, \dots, 6\}$  and the gains  $l_j$ ,  $j \in \{2, 4, 6\}$  satisfy the relations in (49, 65, 80), where  $\mathbf{e}_{r,\max}$ ,  $r \in \{1, 2, 3\}$  are the maximum values of the estimation errors of the disturbance observer given in (27).

**Table 1** Quadrotor's model parameters, desired outputs, and initial outputs

Quadrotor mass	2.25 Kg
Gravitational acceleration	9.81 m/s <sup>2</sup>
Moment of inertia around the inertial $x$ -axis	41.3 g m <sup>2</sup>
Moment of inertia around the inertial $y$ -axis	42.2 g m <sup>2</sup>
Moment of inertia around the inertial $z$ -axis	75.9 g m <sup>2</sup>
Desired position along the $x$ -axis	0.8 m
Desired position along the $y$ -axis	0.8 m
Desired position along the $z$ -axis	10.5 m
Desired heading	30°
Initial position along the $z$ -axis	10 m

#### 4 Simulation results

In this section, the disturbance observer-based command-filtering backstepping controller is implemented and applied to the quadrotor model in simulation. The quadrotor's parameters used in the simulations are listed in Table 1. Table 1 shows also the quadrotor's desired position and heading and the nonzero initial states.

Two test scenarios are implemented in this work. The main aim of the first test scenario is to test the robustness of the controller developed in this work, whereas the main target of the second one is to compare the performance of this developed controller to that of the controller developed in [32]. Although the singular perturbation theory, proving the boundedness of all the tracking errors in [32], is not used in this work due to the discontinuity of the developed controller, the tracking errors are found to be bounded in the following test scenarios by appropriately tuning the gains of the proposed controller.

In the first test scenario, the considered disturbances occur due to two main contributions. The first contribution is the drag force due to wind which is generated by combining constant wind, discrete wind gust model, and Dryden wind turbulence model. The constant wind velocities are chosen to be  $v_{x,\text{constant}} = -4$  m/s,  $v_{y,\text{constant}} = -4$  m/s and  $v_{z,\text{constant}} = -2$  m/s. Two wind gusts occur whose parameters are given in Tables 2 and 3. The parameter  $W_6$  of the Dryden wind is given by  $W_6 = 20$  m/s. The second contribution is the disturbing forces and moments due to partial actuator fail-

**Table 2** First discrete wind gust parameters

Initial time	10 s
Final time	15 s
Initial $x$ -axis velocity	0 m/s
Final $x$ -axis velocity	-4 m/s
Initial $y$ -axis velocity	0 m/s
Final $y$ -axis velocity	-4 m/s
Initial $z$ -axis velocity	0 m/s
Final $z$ -axis velocity	-2 m/s

**Table 3** Second discrete wind gust parameters

Initial time	20 s
Final time	25 s
Initial $x$ -axis velocity	-4 m/s
Final $x$ -axis velocity	-8 m/s
Initial $y$ -axis velocity	-4 m/s
Final $y$ -axis velocity	-8 m/s
Initial $z$ -axis velocity	-2 m/s
Final $z$ -axis velocity	-4 m/s

ure in which the front rotor is simulated to lose 40% of its effectiveness after 30 s.

The disturbing forces and moments affecting the quadrotor during flight along the inertial axes are shown in Fig. 1. The magnitude of the disturbing forces increase over time from  $t = 0$  until  $t = 30$  due to the corresponding increase in the wind velocity. All the disturbing moments from  $t = 0$  s to  $t = 30$  s are zero because the disturbing moments occur only due to actuator failure that takes place at  $t = 30$  s. Moreover, the disturbing moment around the inertial axis  $X_I$  is always equal to zero because the control input  $U_2$  is not affected by the failure of the front rotor. The disturbance's sudden changes at  $t = 30$  s occur because the partial actuator failure happens at this instant.

The disturbance observer estimation errors of the disturbing forces and moments are shown in Fig. 2. The maximum errors of the disturbing force estimates do not exceed 1N along the inertial  $X_I$  and  $Y_I$  axes and reaches 2.5N along the inertial  $Z_I$  axis. The maximum error along the  $Z_I$  axis is higher due to the partial actuator failure occurring at  $t = 30$  s. The maximum errors of the disturbing moment estimates occur once the actuator failure happens because the estimates of

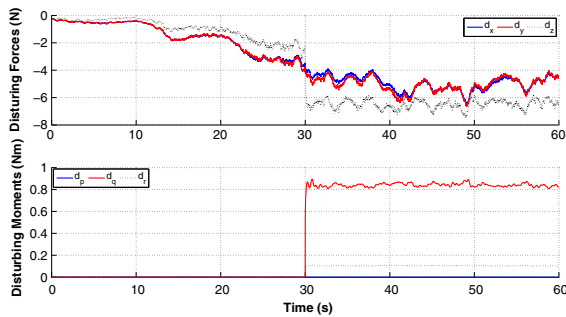


**Fig. 1** Test scenario 1: disturbing forces and moments

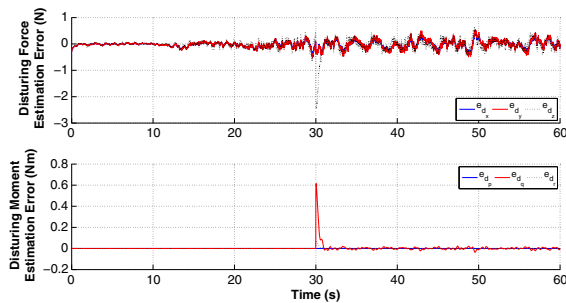


**Fig. 2** Test scenario 1: disturbance observer estimation error

**Table 4** Controller gains

Gain	Value	Gain	Value
$L_d$	$4I_{6 \times 6}$	$l_2$	1
$l_4$	20	$l_6$	2
$k_1$	1	$k_2$	6
$k_3$	15	$k_4$	20
$k_5$	1	$k_6$	2
$a_{10}$	1	$a_{11}$	2
$a_{20}$	25	$a_{21}$	10
$a_{30}$	64	$a_{31}$	16
$a_{40}$	400	$a_{41}$	40
$a_{50}$	1	$a_{51}$	2
$a_{60}$	25	$a_{61}$	10

the disturbing moments are equal to zero at this instant. Based on the maximum values of these errors, the gains  $l_2$ ,  $l_4$ , and  $l_6$  of the discontinuous terms in the control law are chosen as shown in Table 4.

The quadrotor position and attitude response are shown in Figs. 3 and 4. The control signals provided by the controller are shown in Fig. 5. The gains of the backstepping controller are shown in Table 4. As shown in Figs. 3 and 4, the position and heading errors almost

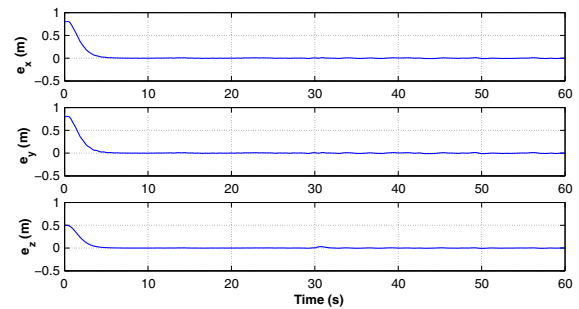


**Fig. 3** Test scenario 1: quadrotor's position errors

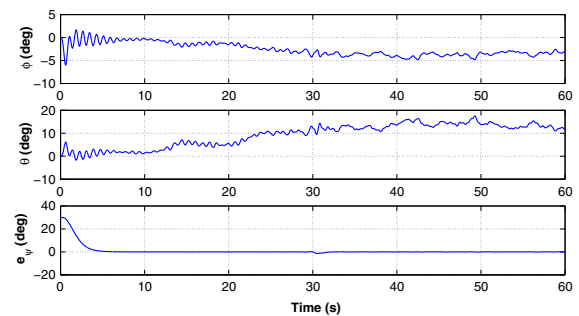


**Fig. 4** Test scenario 1: quadrotor's roll and pitch trajectories and heading error

converge to zero even in the presence of the applied disturbances. The tracking errors start from high initial values due to the difference between the desired output values and the quadrotor initial conditions. In addition, it can be observed from Fig. 4 that the mean values of the roll and pitch angles are not zero since thrust forces along the  $X_I$  and  $Y_I$  axes are needed to counteract the disturbing forces. Furthermore, the sudden changes existing in the control inputs  $U_1$ ,  $U_3$  and  $U_4$  at  $t = 30$  s occur due to the partial actuator failure. The reason why the control inputs in Fig. 5 are continuous is that all of the occurrences of the  $sgn$  function in the control laws are replaced by the  $sat$  function. To justify this replacement, the quadrotor's output tracking errors and control signals using the  $sgn$  function are shown in Figs. 6 and 7 respectively. By comparing the results of the two simulation runs, it is obvious that the quadrotor's output response in both cases is similar with a chatter-free control signal in the case of the  $sat$  function as shown by comparing Figs. 5 and 7. It is worth mentioning that in the case of the  $sgn$  function, some oscillations occur in the output tracking errors. The control input chattering and the output tracking



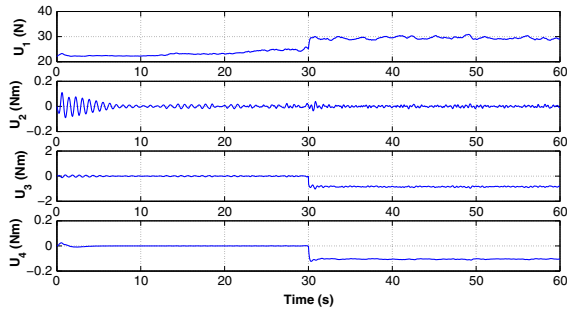


**Fig. 5** Test scenario 1: quadrotor's control inputs

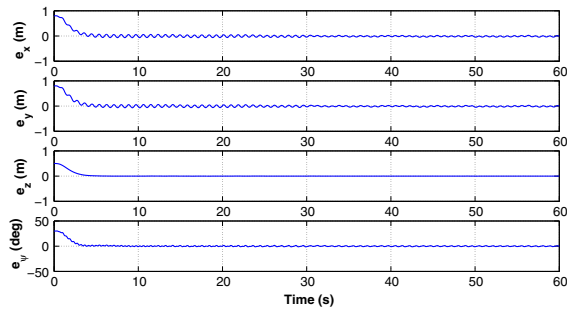


**Fig. 6** Test scenario 1: quadrotor's output errors (using *sgn* function)

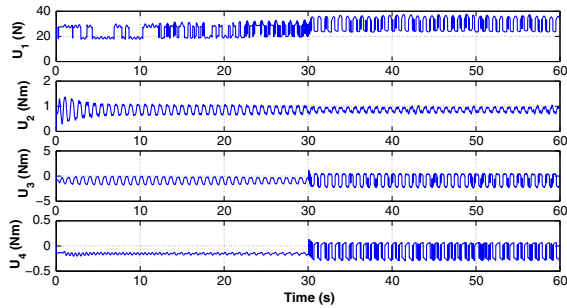


**Fig. 7** Test scenario 1: quadrotor's control inputs (using *sgn* function)

error oscillation make the application of the proposed controller with the *sgn* function impractical.

In the second test scenario, the disturbances due to wind and partial actuator failure are disabled. Instead, rotor dynamics are activated and considered as unmodeled dynamics. The dynamics of each rotor are represented by a first-order low-pass filter with a time constant  $\tau = 20$  and a unity DC gain. The quadrotor's parameters, the quadrotor's initial conditions and the proposed controller gains are selected to be the same as in Tables 1 and 4. The quadrotor's desired

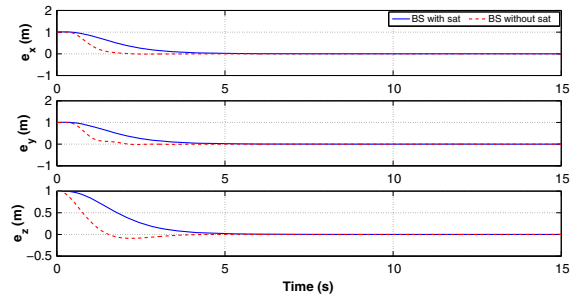


**Fig. 8** Test scenario 2: quadrotor position errors

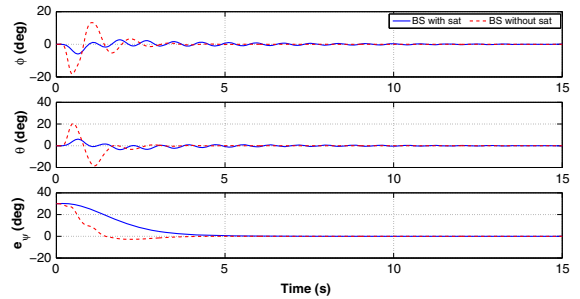


**Fig. 9** Test scenario 2: quadrotor roll and pitch trajectories and yaw error

set-points are selected to be  $\mathbf{x}_{1d} = [1 \text{ m}, 1 \text{ m}]^T$  and  $\mathbf{x}_{5d} = [11 \text{ m}, 30^\circ]^T$ . The gains of the controller in [32] are selected to be the same as those of the controller developed in this paper except for the disturbance observer gains which are chosen to be  $\mathbf{L}_d = 20\mathbf{I}_{6 \times 6}$  instead of  $\mathbf{L}_d = 4\mathbf{I}_{6 \times 6}$ . Since the main difference between the two controllers is the existence of the saturation function in the controller developed in this work, this controller is denoted as the backstepping controller with saturation functions (BS with sat), whereas the other controller is called the backstepping controller without saturation functions (BS without sat).

The quadrotor's output error as well as the roll and pitch angles in the case of both controllers is shown in Figs. 8 and 9. In addition, the control signals provided by both controllers are shown in Fig. 10. As shown in Fig. 8 and the last figure in Fig. 9, the tracking errors in the case of the controller in [32] converge faster than those of the controller developed in this work. This is due to the low-pass filters  $H_1(s)$  and  $H_5(s)$  through which the reference signals propagate. Consequently, the overshoots of the roll and pitch angles in the case of the controller in [32] are higher than those of the newly developed controller in this paper as shown in Fig. 9.

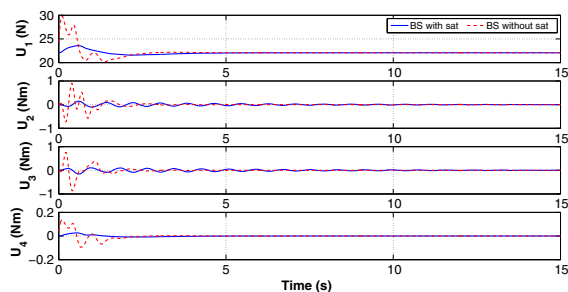


**Fig. 10** Test scenario 2: quadrotor control inputs

Finally, as shown in Fig. 10, the control inputs of the controller in [32] are found to be more aggressive than those of the controller developed in this paper.

It is worth mentioning that, when the disturbance observer gains of the controller in [32] are chosen as  $\mathbf{L}_d = 4\mathbf{I}_{6 \times 6}$ , the controller does not work properly and the tracking errors diverge. This is because the rotor dynamics are considered as fast time-varying disturbances which require fast disturbance observer dynamics to reduce the ignored effect of the disturbance observer estimation errors. On the other side, the controller developed in this work works properly even when choosing low disturbance observer gains because the disturbance observer estimation errors are handled using the saturation function which is not used in the controller in [32].

## 5 Conclusion

In this paper, a model-based nonlinear controller is developed to control the quadrotor in the presence of both constant and time-varying disturbances. The controller is designed using the backstepping approach and the Lyapunov stability theory. The backstepping controller is augmented with a disturbance observer to attenuate the effect of disturbances affecting the quadrotor during flight. To ensure the negative definiteness of the Lyapunov function derivatives, discontinuous terms are added to the control law. The derivatives of the virtual control inputs of the backstepping controller are computed using the command-filtering approach to overcome the complex derivation of these derivatives and to avoid differentiating the discontinuous terms. The developed controller does not utilize any disturbance model. The proposed controller is implemented and applied to a quadrotor model in simula-

tion. Disturbances are generated using a wind model, partial actuator failure, and unmodeled rotor dynamics. The simulation results show the effectiveness of the designed controller.

## References

1. Aboudonia, A., El-Badawy, A., Rashad, R.: Disturbance observer-based feedback linearization control of an unmanned quadrotor helicopter. *Proc. Inst. Mech. Eng. Part I J. Syst. Control Eng.* **230**(9), 877–891 (2016)
2. Åström, K.J., Wittenmark, B.: *Adaptive Control*. Courier Corporation, North Chelmsford (2013)
3. Besnard, L., Shtessel, Y.B., Landrum, B.: Control of a quadrotor vehicle using sliding mode disturbance observer. In: *American Control Conference, 2007. ACC'07*, pp. 5230–5235. IEEE (2007)
4. Bouabdallah, S., Noth, A., Siegwart, R.: PID vs LQ control techniques applied to an indoor micro quadrotor. In: *2004 IEEE/RSJ International Conference on Intelligent Robots and Systems, 2004 (IROS 2004)*. Proceedings, vol. 3, pp. 2451–2456. IEEE (2004)
5. Bouabdallah, S., Siegwart, R.: Backstepping and sliding-mode techniques applied to an indoor micro quadrotor. In: *Proceedings of the 2005 IEEE International Conference on Robotics and Automation, 2005. ICRA 2005*, pp. 2247–2252. IEEE (2005)
6. Castaldi, P., Mimmo, N., Naldi, R., Marconi, L.: Robust trajectory tracking for underactuated VTOL aerial vehicles: Extended for adaptive disturbance compensation. In: *Proceedings of 19th IFAC World Congress*, vol. 19, pp. 3184–3189 (2014)
7. Chen, F., Lei, W., Zhang, K., Tao, G., Jiang, B.: A novel nonlinear resilient control for a quadrotor UAV via backstepping control and nonlinear disturbance observer. *Nonlinear Dyn.* **85**(2), 1281–1295 (2016)
8. Chen, W.H., Yang, J., Guo, L., Li, S.: Disturbance-observer-based control and related methods: an overview. *IEEE Trans. Ind. Electron.* **63**(2), 1083–1095 (2016)
9. Choi, I.H., Bang, H.C.: Adaptive command filtered backstepping tracking controller design for quadrotor unmanned aerial vehicle. *Proc. Inst. Mech. Eng. Part G J. Aerosp. Eng.* **226**(5), 483–497 (2012)
10. Farrell, J., Polycarpou, M., Sharma, M., Dong, W., et al.: Command filtered backstepping. *IEEE Trans. Autom. Control* **54**(6), 1391–1395 (2009)
11. Fernando, T., Chandiramani, J., Lee, T., Gutierrez, H.: Robust adaptive geometric tracking controls on so (3) with an application to the attitude dynamics of a quadrotor UAV. In: *50th IEEE Conference on Decision and Control and European Control Conference (CDC-ECC)*, pp. 7380–7385. IEEE (2011)
12. Guo, B.Z., Zhao, Z.L.: On convergence of the nonlinear active disturbance rejection control for mimo systems. *SIAM J. Control Optim.* **51**(2), 1727–1757 (2013)
13. Han, J.: From PID to active disturbance rejection control. *IEEE Trans. Ind. Electron.* **56**(3), 900–906 (2009)

14. Hancer, C., Oner, K.T., Sirimoglu, E., Cetinsoy, E., Unel, M.: Robust hovering control of a quad tilt-wing UAV. In: IECON 2010-36th Annual Conference on IEEE Industrial Electronics Society, pp. 1615–1620. IEEE (2010)
15. Hoblit, F.M.: Gust Loads on Aircraft: Concepts and Applications. AIAA, Reston (1988)
16. Huang, M., Xian, B., Diao, C., Yang, K., Feng, Y.: Adaptive tracking control of underactuated quadrotor unmanned aerial vehicles via backstepping. In: American Control Conference (ACC), pp. 2076–2081. IEEE (2010)
17. Khalil, H.K.: Nonlinear Systems. Prentice-Hall, New Jersey (1996)
18. Li, J., Li, Y.: Dynamic analysis and PID control for a quadrotor. In: International Conference on Mechatronics and Automation (ICMA), pp. 573–578. IEEE (2011)
19. Li, S., Yang, J., Chen, W.H., Chen, X.: Disturbance Observer-Based Control: Methods and Applications. CRC Press, Cambridge (2014)
20. Madani, T., Benallegue, A.: Backstepping control for a quadrotor helicopter. In: IEEE/RSJ International Conference on Intelligent Robots and Systems, pp. 3255–3260. IEEE (2006)
21. Madani, T., Benallegue, A.: Backstepping sliding mode control applied to a miniature quadrotor flying robot. In: 32nd Annual Conference on IEEE Industrial Electronics, IECON 2006, pp. 700–705. IEEE (2006)
22. Madani, T., Benallegue, A.: Control of a quadrotor mini-helicopter via full state backstepping technique. In: 45th IEEE Conference on Decision and Control, pp. 1515–1520. IEEE (2006)
23. Madani, T., Benallegue, A.: Backstepping control with exact 2-sliding mode estimation for a quadrotor unmanned aerial vehicle. In: IEEE/RSJ International Conference on Intelligent Robots and Systems, 2007. IROS 2007, pp. 141–146. IEEE (2007)
24. Madani, T., Benallegue, A.: Sliding mode observer and backstepping control for a quadrotor unmanned aerial vehicles. In: American Control Conference, 2007. ACC'07, pp. 5887–5892. IEEE (2007)
25. Mahony, R., Kumar, V., Corke, P.: Multirotor aerial vehicles: modeling, estimation, and control of quadrotor. IEEE Robot. Autom. Mag. **19**(3), 20–32 (2012). doi:[10.1109/MRA.2012.2206474](https://doi.org/10.1109/MRA.2012.2206474)
26. Ohishi, K., Nakao, M., Ohnishi, K., Miyachi, K.: Microprocessor-controlled dc motor for load-insensitive position servo system. IEEE Trans. Ind. Electron. **1**, 44–49 (1987)
27. Palunko, I., Fierro, R.: Adaptive control of a quadrotor with dynamic changes in the center of gravity. IFAC Proc. Vol. **44**(1), 2626–2631 (2011)
28. Pounds, P., Mahony, R., Corke, P.: Modelling and control of a large quadrotor robot. Control Eng. Pract. **18**(7), 691–699 (2010). doi:[10.1016/j.conengprac.2010.02.008](https://doi.org/10.1016/j.conengprac.2010.02.008)
29. Ran, M., Wang, Q., Dong, C.: Active disturbance rejection control for uncertain nonaffine-in-control nonlinear systems. IEEE Trans. Autom. Control (2016)
30. Ran, M., Wang, Q., Dong, C.: Stabilization of a class of nonlinear systems with actuator saturation via active disturbance rejection control. Automatica **63**, 302–310 (2016)
31. Rashad, R., Aboudonia, A., El-Badawy, A.: Backstepping trajectory tracking control of a quadrotor with disturbance rejection. In: XXV International Conference on Information, Communication and Automation Technologies (ICAT), pp. 1–7. IEEE (2015)
32. Rashad, R., Aboudonia, A., El-Badawy, A.: A novel disturbance observer-based backstepping controller with command filtered compensation for a MIMO system. J. Frankl. Inst. **353**(16), 4039–4061 (2016)
33. Sadeghzadeh, I., Mehta, A., Zhang, Y., Rabbath, C.A.: Fault-tolerant trajectory tracking control of a quadrotor helicopter using gain-scheduled PID and model reference adaptive control. In: Annual Conference of the Prognostics and Health Management Society, vol. 2 (2011)
34. Schreier, M.: Modeling and adaptive control of a quadrotor. In: International Conference on Mechatronics and Automation (ICMA), pp. 383–390. IEEE (2012)
35. Sun, H., Li, S., Yang, J., Guo, L.: Non-linear disturbance observer-based back-stepping control for airbreathing hypersonic vehicles with mismatched disturbances. IET Control Theory Appl. **8**(17), 1852–1865 (2014)
36. Wang, H., Chen, M.: Sliding mode attitude control for a quadrotor micro unmanned aircraft vehicle using disturbance observer. In: Guidance, Navigation and Control Conference (CGNCC), 2014 IEEE Chinese, pp. 568–573. IEEE (2014)
37. Waslander, S.L., Wang, C.: Wind disturbance estimation and rejection for quadrotor position control. In: AIAA Infotech@ Aerospace Conference and AIAA Unmanned Unlimited Conference, Seattle, WA (2009)
38. Xu, R., Ozguner, U.: Sliding mode control of a quadrotor helicopter. In: 45th IEEE Conference on Decision and Control, pp. 4957–4962. IEEE (2006)
39. Zhao, S., Dong, W., Farrell, J.A.: Quaternion-based trajectory tracking control of vtol-uavs using command filtered backstepping. In: 2013 American Control Conference, pp. 1018–1023. IEEE (2013)
40. Zuo, Z.: Trajectory tracking control design with command-filtered compensation for a quadrotor. IET Control Theory Appl. **4**(11), 2343–2355 (2010)
41. Zuo, Z.: Adaptive trajectory tracking control design with command filtered compensation for a quadrotor. J. Vib. Control **19**(1), 94–108 (2013)